M. K. Ferber, H. T. Lin, and J. Keiser[1]

Oxidation Behavior of Non-Oxide Ceramics in a High-Pressure, High-Temperature Steam Environment

Reference: Ferber,M. K., Lin, H. T., and Keiser, J., **"Oxidation Behavior of Non-Oxide Ceramics in a High-Pressure, High-Temperature Steam Environment,"** *Mechanical, Thermal and Environmental Testing and Performance of Ceramic Composites and Components, ASTM STP 1392*, M. G. Jenkins, E. Lara-Curzio and S. T. Gonczy, Eds., American Society for Testing and Materials, West Conshohocken, PA, 2000.

Abstract: This paper provides a review of two recent studies undertaken to examine the oxidation behavior of monolithic SiC and SiC-SiC composites in simulated and actual gas turbine environments. In the first study, a high-pressure and high-temperature test facility was used to expose a variety of structural ceramics and ceramic matrix composites to 15% water vapor carried in an air environment at 10 atm of total pressure and 1204°C. The second study involved the exposure of a SiC-SiC combustor liner in an industrial gas turbine for approximately 2300 h at a total pressure of 10 atm and peak liner temperature of 1150°C.

In the two studies microstructural analyses were used to measure the rates of both silica scale formation and SiC recession. These experimentally determined rates were then compared with values predicted from established oxidation/volatilization models. The estimates of the temperature and pressure sensitivities of the oxidation and volatilization rate constants, required for this comparison, were obtained from the literature. For the case of the combustor liner, the recession rate of SiC was well described by the model. However, the predicted rates of scale formation in both studies were significantly lower that the corresponding experimental values. Possible reasons for this discrepancy are addressed.

Keywords: silicon carbide, silicon nitride, ceramic, composite, CFCC, paralinear oxidation, microstructural analysis

Introduction

Monolithic silicon nitride and silicon carbide ceramics as well as continuous fiber reinforced ceramics are leading candidates for use as high-temperature, structural components in advanced gas turbines [*1-5*]. These materials offer the following advantages over their metallic counterparts: (1) low density, (2) refractoriness, (3) adequate short-term strength, (4) good corrosion and oxidation resistance at intermediate to high oxygen partial pressures, and (5) their shape fabrication technology is mature.

The gas turbine components, where ceramics could be inserted, include combustors,

[1] Research Staff, Oak Ridge National Laboratory, P. O. Box 2008, MS 6069, Oak Ridge, TN, 37831-6069.

transition sections, hot gas ducts, vanes, and turbine blades. All but turbine blades are classified as stationary components. The materials for the stationary component require moderate hot strength, good thermal shock resistance, and shape stability. The rotating turbine blades call for higher strength materials and tolerance to impact. These components must also operate reliably for extended periods (>30 000 h for industrial gas turbines).

Because the aforementioned materials are typically fabricated from SiC or Si_3N_4, their long-term reliability depends upon the formation of a passive oxide layer. This situation arises when the diffusion of the oxidant controls the oxidation and the rate of scale growth decreases with time in accordance with parabolic rate kinetics. Unfortunately, the gas turbine environment includes water vapor at pressures well in excess of 1 atmosphere. For a given temperature, oxidation of both silicon nitride and silicon carbide is increased by (1) the replacement of oxygen by water vapor and (2) an increase in the pressure of the oxidant [*6-8*]. In addition, the high velocities and presence of water in the environment can lead to the volatilization of the normally protective silica layer. The modeling of this behavior is discussed in the next section.

Paralinear Model

The competing processes of scale formation and scale volatilization ultimately lead to the linear recession of the ceramic substrate (paralinear kinetics).[2] For the case of SiC, the total change in weight is the sum of two components, Δw_1, the increase in weight arising from the oxidation of SiC, and Δw_2, the loss in weight arising from volatilization of the silica scale. The resulting paralinear kinetics are described by the two equations

$$t = (\alpha^2 k_p/(2k_l^2)) [- 2k_l\Delta w_1/(\alpha k_p) - \ln (1 - 2k_l\Delta w_1/(\alpha k_p))] \qquad (1a)$$

and

$$\Delta w_2 = -\beta k_l t \qquad (1b)$$

where t is the time, k_p is the parabolic oxidation rate constant, and k_l is the linear rate constant for silica scale volatilization. The values of the constants, α and β, depend upon the molecular weights (MW) of the oxidation species. In the case of SiC, these constants are calculated from the following expressions

$$\alpha = MW(SiO_2)/[MW(O_2) - MW(C)] \qquad (2a)$$

and

$$\beta = MW(SiC)/MW(SiO_2) \qquad (2b)$$

To apply these expressions to the experimental data described in this paper, the temperature and pressure sensitivities of k_l and k_p must first be known. As discussed in Ref *8*, volatilization of silica in the presence of water vapor occurs primarily by the formation of a gaseous $Si(OH)_4$ species. For lean burn conditions examined in Ref *8*, k_l for a number of SiC based materials was found to be well described by the expression,

---

[2] The discussion that follows including the derivations of Eqs 1 through 9 is based upon the work in Ref *6*.

$$\beta\, k_l\ (mg/cm^2\ h) = 2.04 \exp(-108\ kJ/mole/RT)\ v^{1/2}\ P_{total}^{\ 3/2}, \qquad (3)$$

where v is the gas velocity in m/sec, T is the absolute temperature (K), and P_{total} is the total pressure in atmospheres. The β term must be included in Eq 3 in order to convert the silica recession rate, represented by k_l, to the SiC recession rate.

The pressure and temperature sensitivities of k_p were recently measured in Ref *7*. The data are reproduced in Figure 1. For temperatures above 1100°C, the pressure dependency is to a first approximation independent of T. Therefore, k_p can be represented by the expression

$$k_p = A \exp(-Q/RT)\ P_{H2O}^{\ N} \qquad (4)$$

where Q is the activation energy and N is a constant. A multi-linear regression analysis was used to simultaneously estimate A, Q, and N. The k_p data at 1100°C were not used in this fitting procedure due to a possible change in oxidation mechanism at this temperature [*7*]. The lines in Figure 1, which illustrate the best fit to the data, are described the equation

$$k_p\ (mg^2/cm^4\ h) = 0.22 \exp(-56.7\ kJ/mole\ /RT)\ P_{H2O}^{\ 0.8} \qquad (5)$$

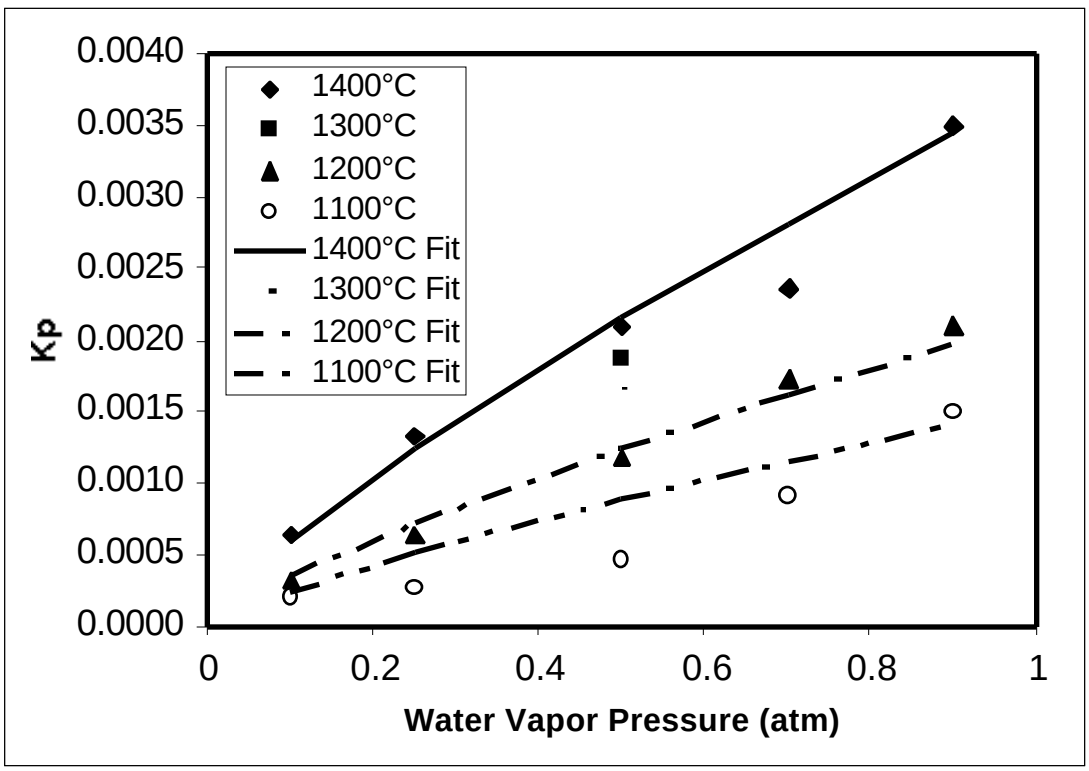

Figure 1 Pressure and temperature sensitivities of K_p generated from data found in [7]. The units for K_p are (mg^2/cm^4 h). The lines represent the multi-linear regression fit of the data to the model described in the text.

Equations 1 through 5 describe paralinear kinetics in terms of the specific weight changes.

The thickness of the silica scale, X_{SiO2}, can be related to Δw_1 via the expression

$$X_{SiO2} = \Delta w_1 \, \alpha / \rho_{SiO2} \qquad (6)$$

where ρ_{SiO2} is the density of the scale. Likewise, the thickness of the scale that has volatilized, $X_{SiO2(v)}$, is given by

$$X_{SiO2(v)} = -\Delta w_2 / \beta / \rho_{SiO2}. \; (\Delta w_2 < 0) \qquad (7)$$

Finally, the thickness of the SiC recession zone is related to the total thickness of the silica scale through the expression

$$X_{SiC} = (X_{SiO2} + X_{SiO2(v)}) \, \beta \, \rho_{SiO2} / \rho_{SiC} \qquad (8a)$$

or using Eqs 6 and 7

$$X_{SiC} = (\Delta w_1 \, \alpha \, \beta - \Delta w_2) / \rho_{SiC} \qquad (8b)$$

where ρ_{SiC} is the density of the SiC. Using these equations, the relationship between silica scale thickness and time is

$$t = (k_p/(2k_l^2)) \, [- 2k_l X_{SiO2}/(k_p) - \ln (1 - 2k_l X_{SiO2}/(k_p))] \qquad (9)$$

where k_p and k_l are the parabolic and volatilization rate constants, respectively, expressed in terms of thickness rather than specific weight.

In accordance with the paralinear model, Δw_1 and X_{SiC} increase to constant values at which time the generation of the silica scale by oxidation is balanced exactly by the loss of the scale due to volatilization. The steady-state thickness of the scale, X_{SiO2} (ss), is given by $(k_p/(2k_l))$. The total weight of the system, $\Delta w_1 + \Delta w_2$, continues to decrease due the linear dependence of Δw_2 upon time. The recession of the SiC also continues in accordance with Eq 8.

A major objective of this research was to compare the SiC recession and oxidation rates predicted from the paralinear model described above with available experimental data. In this case the experimental data were obtained from two recent studies [*9*, *10*] undertaken to examine oxidation behavior of SiC based materials in simulated and actual gas turbine environments. In the first study [9], a high-pressure and temperature test facility (HPTTF) was used to expose a variety of structural ceramics and ceramic matrix composites to steam. The second study involved the exposure of SiC-SiC combustor liners (Figure 2) in field tests of a Centaur 50S natural gas turbine.[3]

Experimental Procedure

The materials investigated in this paper are summarized in Table 1. The composite materials were exposed as coupons in the HPTTF and as combustor liners in the field test of an industrial gas turbine. In most cases, a dense chemical vapor deposited (CVD) SiC seal coat was applied to surfaces of the SiC-SiC specimens. The monolithic sintered-alpha silicon carbide was exposed only in the HPTTF.

---

[3] Solar Turbines, Dan Diego, CA.

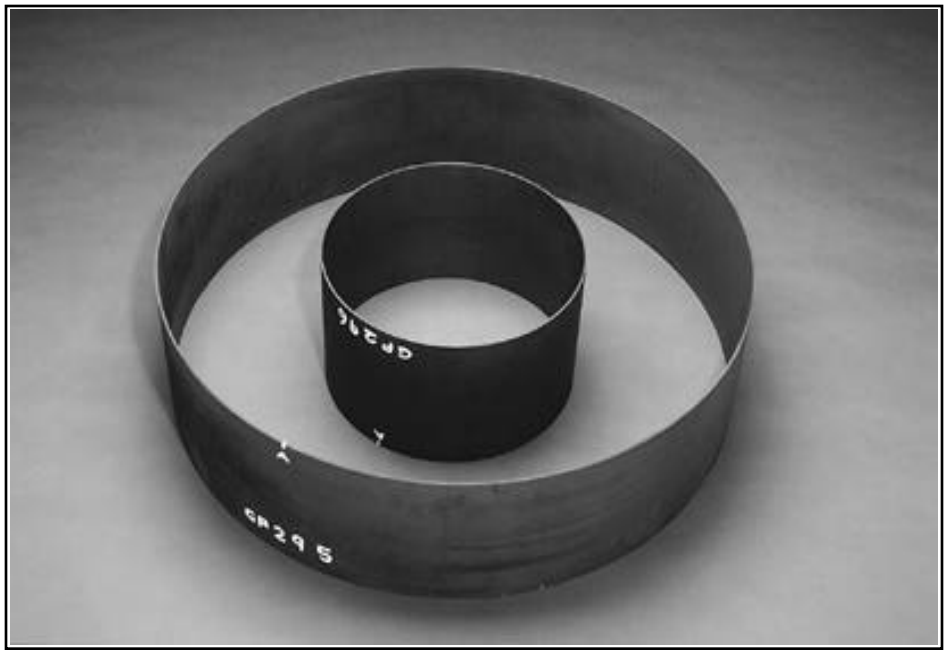

Figure 2 SiC-SiC combustor liner utilized in a field test of Solar Turbine's Centaur 50S Natural Gas Turbine. The diameters of the inner and outer liners are 330 mm (13 in) and 762 mm (30 in), respectively.

Table 1-Summary of materials examined in this program.

Material	Supplier	Comments
SA SiC	Carborundum Company Niagara Falls, NY 14302-0832	Exposed in the HPTTF
Enhanced SiC/SiC-PyC-CG-Nicalon	AlliedSignal Composites, Inc. P.O. Box 9559 Newark, DE 19714-9559	Exposed in the HPTTF Liner field-tested for 1000 h
Enhanced SiC/SiC-PyC-Hi-Nicalon	AlliedSignal Composites, Inc. P.O. Box 9559 Newark, DE 19714-9559	Exposed in the HPTTF Liner field-tested for 2250 h
Enhanced SiC/SiC-BN-Hi-Nicalon	AlliedSignal Composites, Inc. P.O. Box 9559 Newark, DE 19714-9559	Exposed in the HPTTF Liner field-tested for 2250 h

An overview of the high-temperature, high-pressure test facility is shown in Figure 3. The primary components of the test system were the furnace, ceramic containment tubes, and gas supply system. The top-loading furnace was capable of 1550°C operation and had external dimensions of about 1.2 m on each side with a hot zone that was approximately 25 cm wide by 41 cm deep by 66 cm high. The top cover of the furnace had six holes. As shown in Figure 3a, each hole accommodated a 8.9 cm OD containment tube (SA SiC). These tubes, which were 1.2 m long, contained the test atmosphere. Approximately 28 cm of the tube extended above the top of the furnace. The tubes were

closed at the end that extends into the furnace and the open end had an expanded section to provide a sealing surface and a means to hold the tube. This expanded section accommodated a stainless steel flange that contained fittings so that a pressurized gas mixture could be fed to and removed from the tubes at pressures up to 20.4 atm (300 psia).

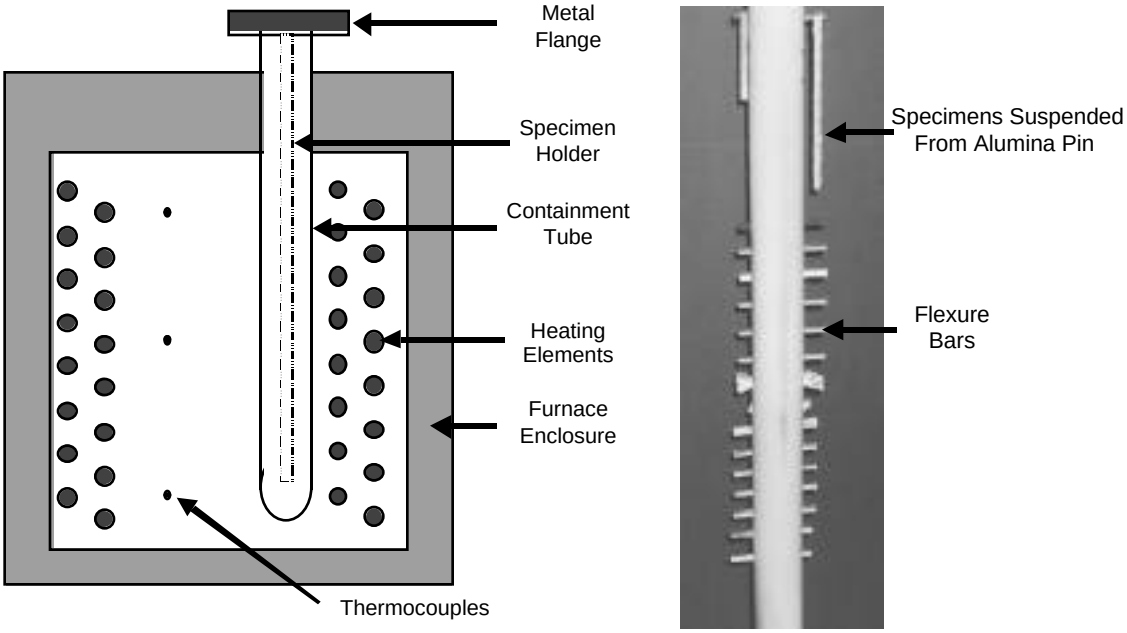

(a) (b)

Figure 3 Key elements of the High-Pressure and Temperature Test Facility (HPTTF) including (a) schematic drawing of pressure containment tube and (b) Aluminum Oxide Specimen Holder.

An aluminum oxide hollow-tube specimen holder (Figure 3b) was suspended within each ceramic containment tube. This tube was approximately 0.9 m in length and 4.5 cm in diameter with a 0.635 cm wall thickness. In order to accommodate the specimens to be exposed, regularly spaced slots were machined into the holder. These slots could accept standard flexure bars 3 by 4 by 50 mm in size. As shown in Figure 3b, larger sized specimens were hung from aluminum oxide pins placed through the machined slots.

The gas supply system permitted a measured amount of bottled gas to be combined with a controlled amount of steam to simulate the atmosphere. For these studies, the flow of air, which was used as the carrier gas, was regulated with a mass flow controller. A pneumatically driven metering pump controlled the supply of high-purity distilled water to the evaporator. The amounts of air and distilled water supplied to the system were manually adjusted to the desired proportions (typically to maintain 15% steam). The gas mixture was fed to each of two SA SiC ceramic containment tubes used in this study.

The effluent gas from the ceramic tubes was conducted to a pneumatically driven back-pressure control valve which was controlled through a feedback loop that incorporated a pressure transducer. Water in the effluent was condensed in an air-cooled coil, collected and the volume measured. The volume of the remaining effluent gas was determined using a calibrated flow meter.

Table 2 lists the environmental test conditions for the HPTTF. Because the gas velocity was low, volatility effects were expected to be negligible in accordance with Eq 3. Specimens in the form of either flexure bars or tensile coupons were exposed for repeated periods of 500 h. In a few instances selected specimens were exposed for a single 100 h test. After a 500 h exposure, each specimen was weighed and measured. Following removal of small sections for microstructural analysis, the specimens were weighed again and then loaded into the specimen hold for the subsequent exposure.

Table 2 Summary of exposure environments considered in this work.

Environment	Pressure (atm) Total/Water Vapor	Test Duration (h)	Velocity (m/s)	T (°C)
HPTTF H_2O in Air [9]	10/1.5	100 500	0.0005	1204
Combustor Liner [10]	10/1.5	2250	61	1150

In the case of the combustor liner field tests, the nominal gas pressure and velocity in the combustor were 10 atm (with 15% water vapor) and 61 m/sec, respectively (Table 2). The peak liner temperature was 1150°C [10]. To date, liners with an accumulated exposure time of 2250 h have been characterized.

In both of the aforemention studies, the measurement of weight changes associated with oxidation and volatilization of the silica scale proved either unreliable in the case of the HPTTF exposure (due to spallation of the scale upon cooling) or impractical in the case of the combustor liner. In order to overcome this problem, scale thickness and SiC recession for the specimens exposed in the HPTTF were measured from polished cross sections using an optical microscope equipped with calibrated x-y stages. The resolution of these measurements was better that 1 µm. In the case of the combustor liners, the rate of recession of the CVD SiC seal coat, which was always present on the as-fabricated liners, was determined by noting the approximate time required for the first breach of the seal coat. The complete penetration of the seal coat was identified during periodic boroscope inspections by the appearance of a white scale. In the present study, the times to breach the seal coats were determined for three liners each having different initial seal coat thicknesses. Consequently a plot of initial thickness versus penetration time was used to estimate the rate of seal coat recession.

Results

HPTTF Data

Scanning electron micrographs of polished cross sections of SA SiC and CVI SiC-SiC materials are shown in Figures 4 and 5, respectively. The scales on both materials consisted of a thick defective (cracked and porous) silica layer, which was identified by x-ray diffraction as cristobalite. In the case of the SiC-SiC composite, a thin amorphous silica layer was present at the surface of the CVD SiC seal coat (Figure 6). The thickness of the amorphous layer stayed constant at 4-6 um throughout the exposure. Two mechanisms may have been responsible for the extensive vertical cracking observed in the silica layer. The first, which occurred at temperature, involved the transformation of the amorphous scale (density = 2.21 g/cm^3) to the crystalline silica (density = 2.37 g/cm^3). The second mechanism, which occurred upon cooling, was the conversion of β cristobalite to α cristobalite. The volume decrease associated with both processes would lead to the

generation of in-plane tensile stresses.

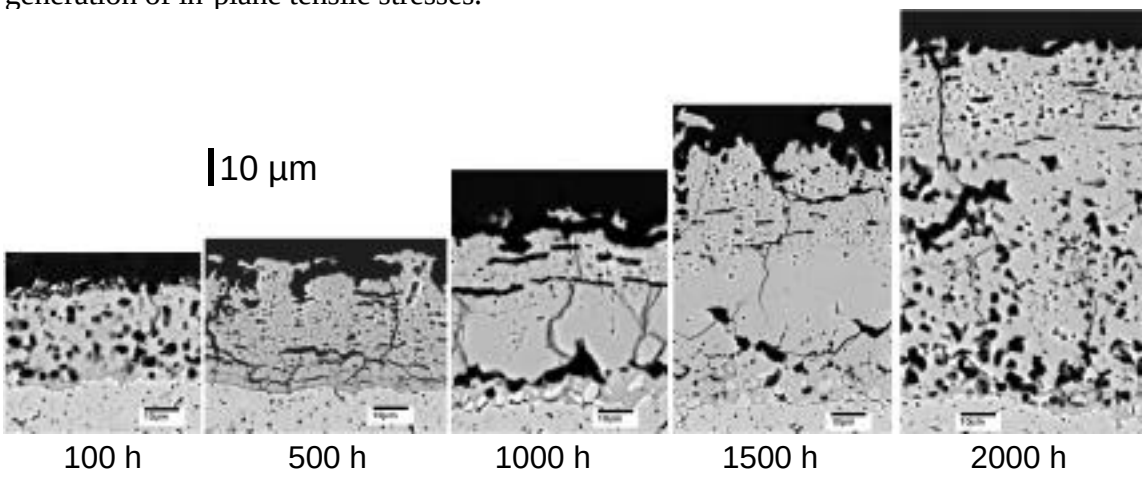

Figure 4 Scanning electron micrographs of a SA SiC specimen exposed in the HPTTF.

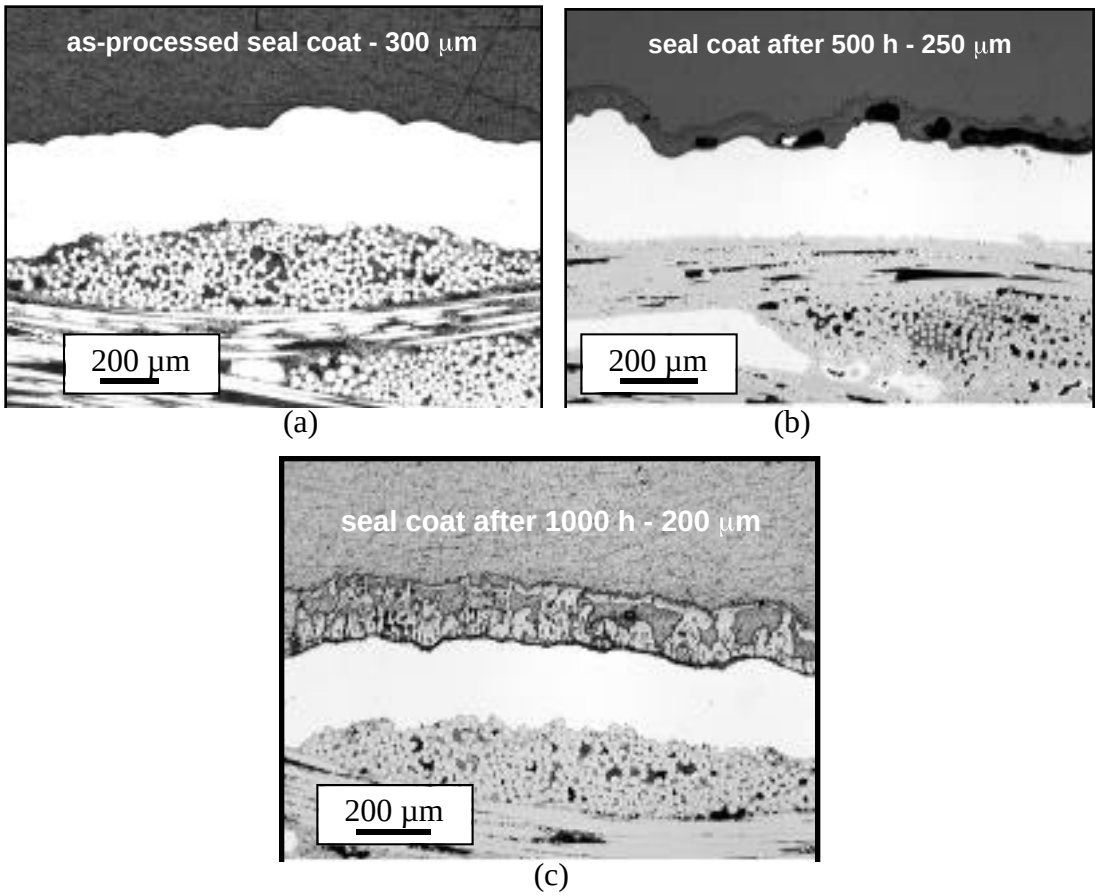

Figure 5. Scanning electron micrographs of a SiC-SiC specimen exposed in the HPTTF for (a) 0, (b) 500, and (c) 1000 h.

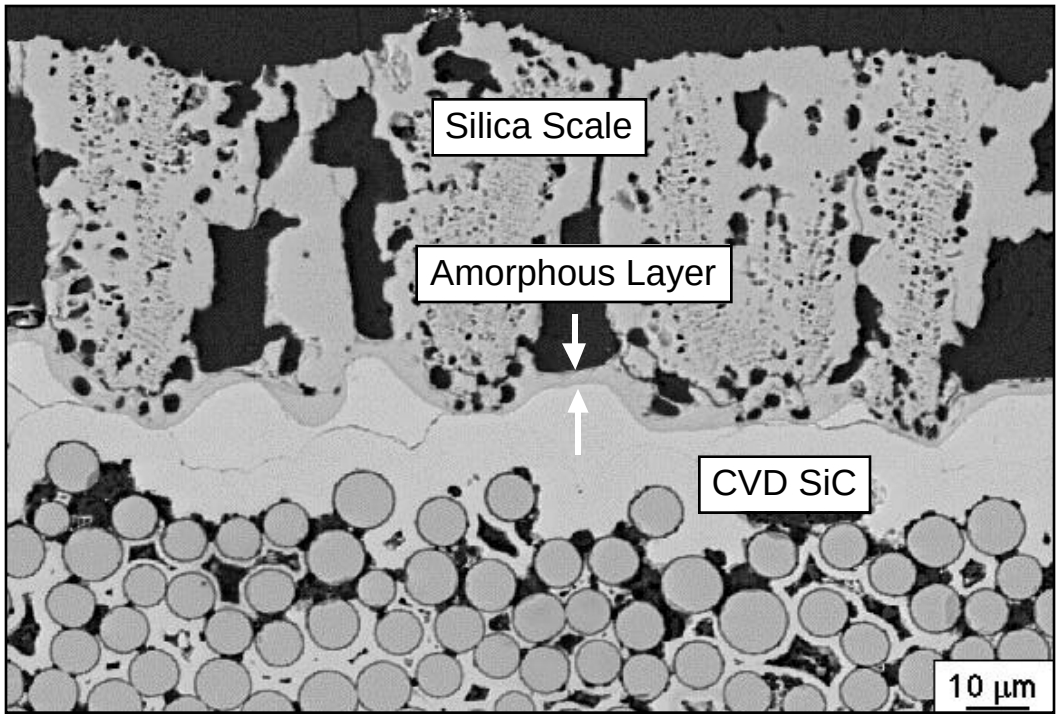

Figure 6 Thin amorphous silica layer.

In addition to the cracks, extensive porosity was also observed. The most likely source of this porosity was the evolution of gas during the oxidation of the SiC. Image analysis of the scale microstructures (excluding the cracks) further revealed that the area fraction of pores increased with time. Given the extensive damage present in the outer silica scale, its effectiveness as a barrier to oxygen (or water vapor) diffusion may have been limited. As discussed below this observation is consistent with the fact that parabolic oxidation rate constant required to fit the experimental oxidation data was much larger than the value predicted from Eq 5.

The recession and oxidation data obtained for the dense SA SiC in the HPTTF exposure are shown in Figure 7 (symbols). Because the gas velocities in the HPTTF are relatively low, volatilization of the silica scale is negligible. As a result, the scale thickness does not reach a steady-state value but continues to increase with time. Using the HPTTF environmental data in Table 2, the values of k_l and k_p were estimated from Eqs. 3 and 5, respectively (see Table 3). These numbers were then used to calculate the silica thickness and SiC recession as a function time in accordance with Eqs 1, 6, 7, and 8. The predicted trends (solid lines in Figure 7) significantly underestimate the experimental data.

It must be emphasized that the extrapolation of the oxidation data in Ref *7* to the conditions in the HPTTF is based upon the assumption that silica scale morphology is independent of environment. Because the scales formed in the HPTTF were heavily damaged, their effectiveness as an oxidation barrier was reduced significantly over that in Ref *7*. This difference may be accounted for by increasing the value of the oxidation rate constant. Although a much better fit is obtained if k_p is increased by a factor of 10 (Figure 8), the predicted curves are parabolic while the actual data exhibit more of a linear dependence upon time. There are number of possible mechanisms that could give rise to linear oxidation (and recession). The first concerns the effectiveness of the silica scale as a

diffusion barrier. In particular, image analysis of the SA SiC micrographs showed that the area fraction of pores increased with time. Assuming that the porosity reduces the effectiveness of the silica as a diffusion barrier, this behavior would counter the tendency for parabolic scale formation. A similar role of porosity has been discussed in Ref [*7*].

Table 3 Summary of rate parameters for the two environments.

Environment	k_p (mg^2/cm^4 h) Eq. 5	k_l (mg/cm^2 h) Eq. 3
HPTTF H_2O in Air	3.0×10^{-3}	3.28×10^{-4}
Gas Turbine Combustor	2.5×10^{-3}	8.2×10^{-2}

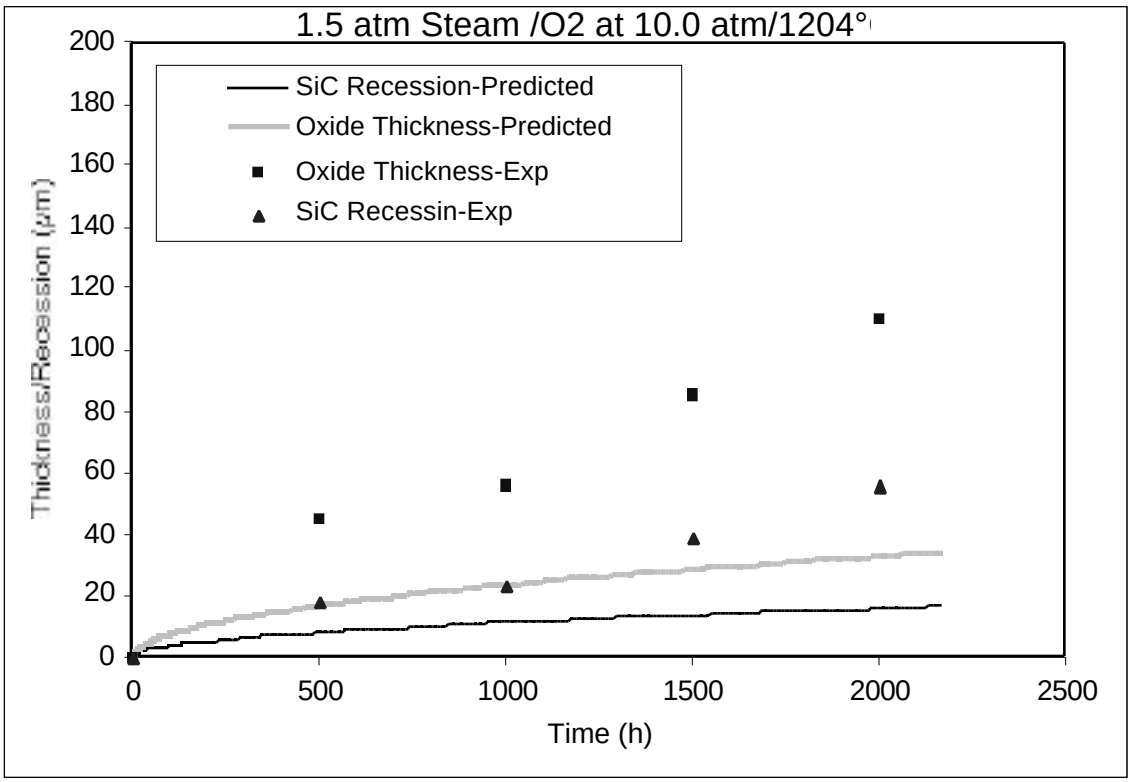

Figure 7 Comparison of SiC recession and oxidation data obtained in the HPTTF with model predictions.

The second mechanism for the linear time dependencies of SiC oxidation and recession in the HPTTF concerns the rate controlling process. As discussed in Ref *11*, oxidation of SiC involves three sequential steps: (1) diffusion of the oxidant to the silica-ceramic interface, (2) oxidation reaction at the interface, and (3) diffusion of the gaseous reaction products from the interface to the free surface. Parabolic oxidation kinetics will only prevail if either Steps 1 or 3 are rate limiting. At ambient pressures the diffusion of the oxidant through the scale is generally assumed to be the slow step. An increase in the

oxidant pressure increases the transport rate through the scale and thus k_p in accordance with Eq 4. If the oxidation reaction (Step 2) is somewhat insensitive to pressure as suggested by limited data in Ref *7*, an increase in oxidant pressure may cause Step 2 to become rate limiting.

Combustor Liner Data

The SiC-SiC combustor liners utilized in the field tests of Solar Turbine's Centaur 50S natural gas turbine had protective CVD SiC seal coats. The combined effects of high water vapor pressure and high gas velocity led to relatively high SiC recession rates. Once the seal coat was breached, a white scale formed quickly due to the extensive oxidation of the underlying composite (Figure 9). The subsequent microstructural analysis of the liner showed that the oxide scale that formed along the surface exposed directly to the combustion environment reached a steady-state thickness of approximately 5 µm (Figure 10). In order to estimate the rate of seal coat recession, the time at which the seal coat was first breached was determined from periodic boroscope inspections of the turbine. It was assumed that the intial breach of the seal coat occurred in the highest temperature region of the liner (taken as 1150°C). Data for three liners having different initial seal coat thicknesses are shown in Figure 11.

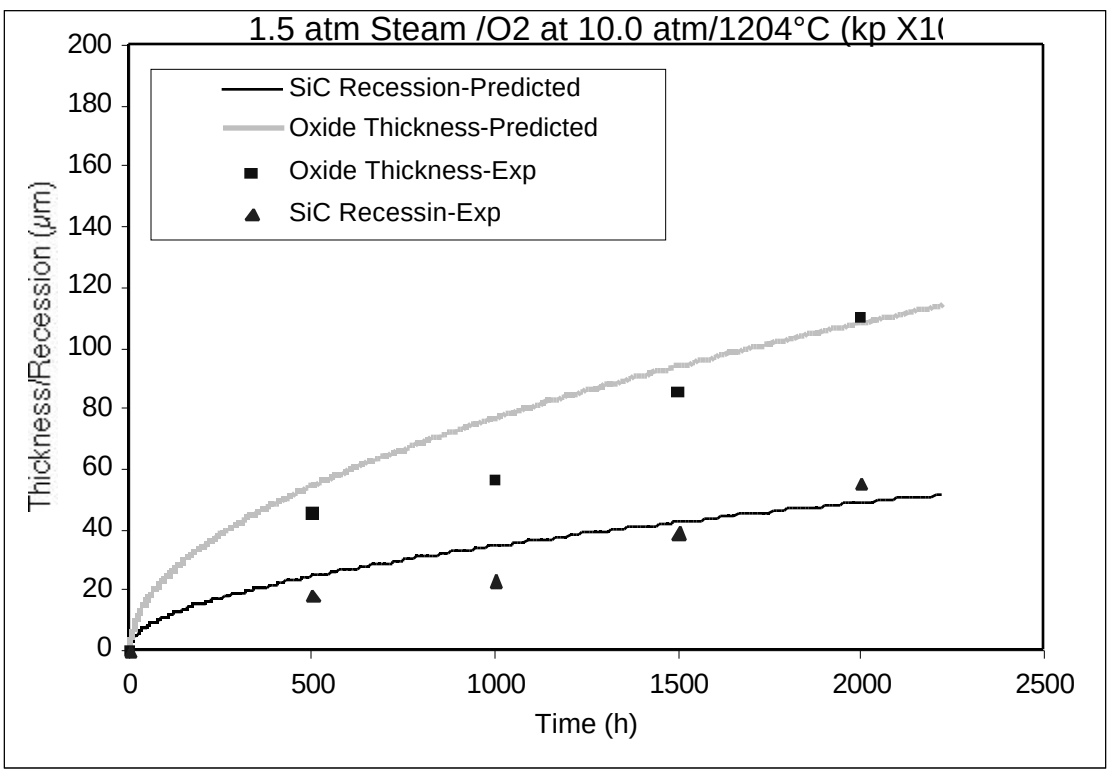

Figure 8 Effect of increasing k_p upon model predictions.

Using the environmental data in Table 2, the values of k_l and k_p were estimated from Eqs 3 and 5, respectively (see Table 3). The predicted SiC recession curve (see

Figure 11) slightly over-predicts the experiment recession data. The most likely reason for this discrepancy is that the combustor liner was not continually operated at the peak conditions given in Table 1. Therefore, the estimated value of k_l, which controls the recession rate in the case of the combustion environment, represents the maximum value rather than an effective average. The steady-state thickness of the silica scale, which was also estimated from the model, was 0.66 µm (Figure 11), which is well below the value measured experimentally. As in the case of the HPTTF results, much better agreement was obtained by increasing k_p by a factor of 10. In this case, the predicted steady-state thickness was 5.5 µm. Because SiC recession is controlled by the k_l value, the predicted recession curve was not affected by increasing k_p.

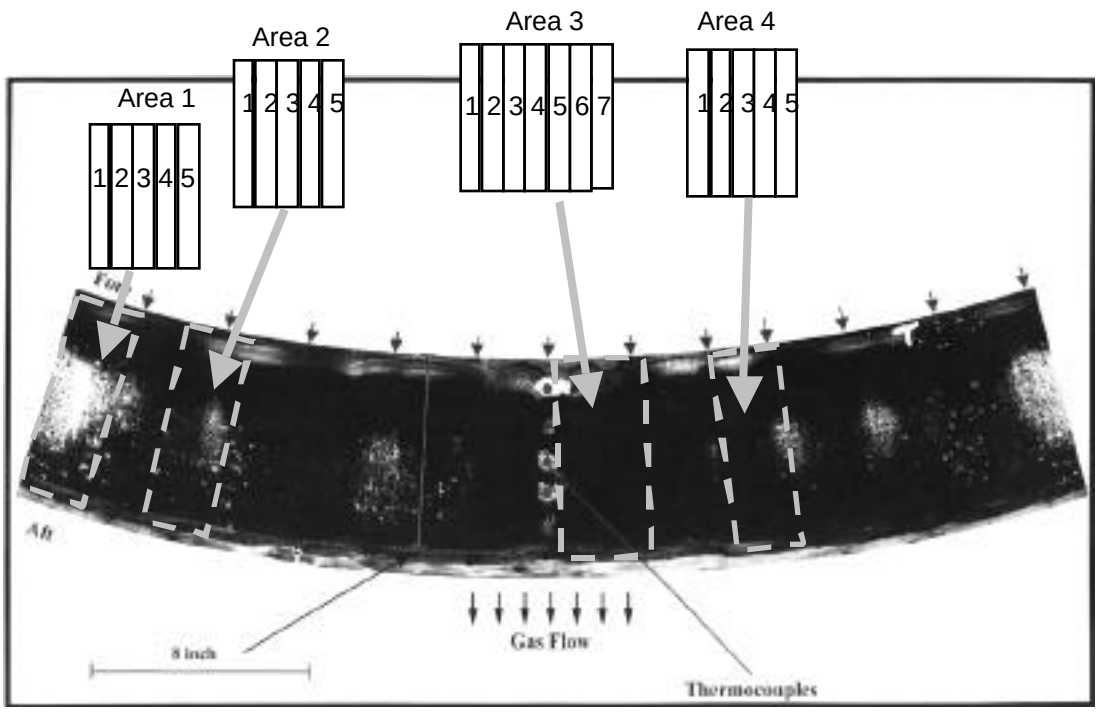

Figure 9 Panoramic view of surface of inner liner exposed for 2250 h. The white patches represent regions in which the seal coat was breached. Strips from 4 areas (designated 1-4) were sectioned for microstructural and mechanical property measurements.

The model may be tested further by predicting the thickness of the oxide scale formed along the internal SiC coated surfaces of the composite. Because these surfaces were isolated from the high gas velocities, volatilization effects were negligible (k_l <<0). As shown in Figure 12, the thickness after 2250 h was approximately 75 µm, which is in fair agreement with the value of 100 µm predicted assuming that k_p is a factor of 10 higher than the value given in Table 3.

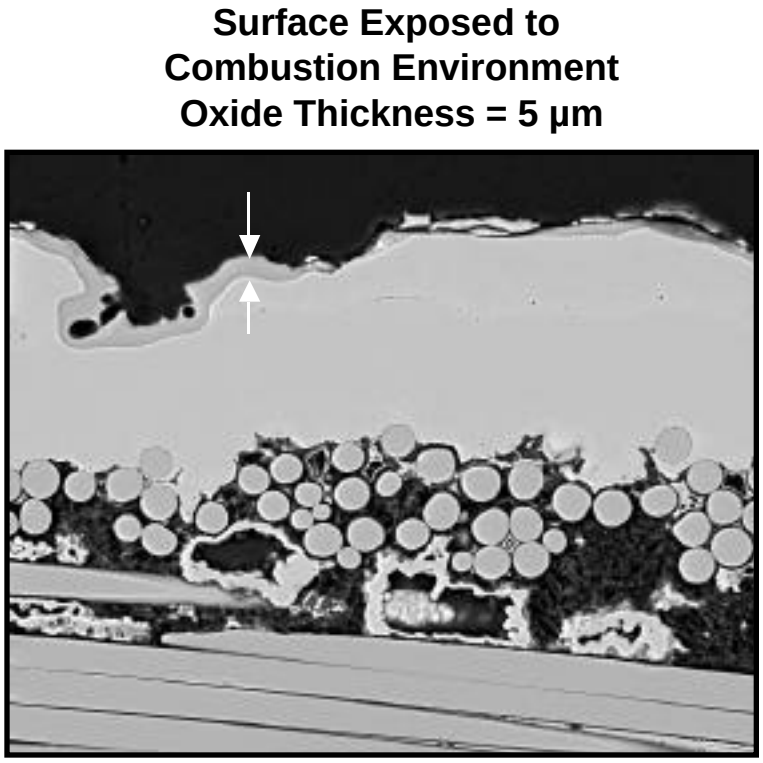

Figure 10 Cross-section of inner liner showing oxide scale on the CVD seal coat.

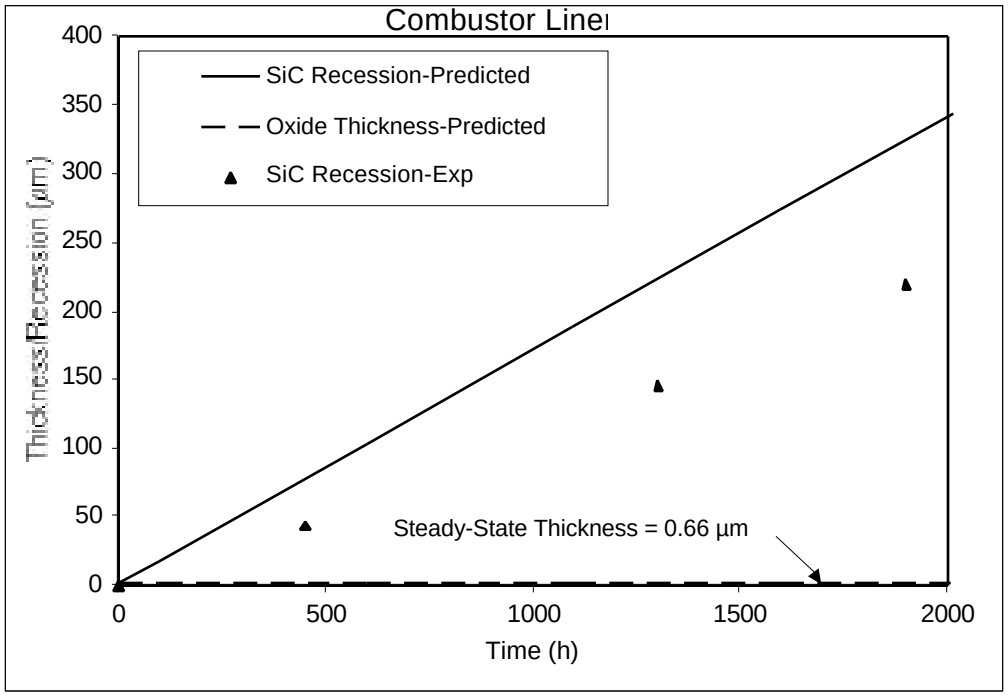

Figure 11 Comparison of CVD SiC recession and oxidation data obtained in the combustion environment with model predictions.

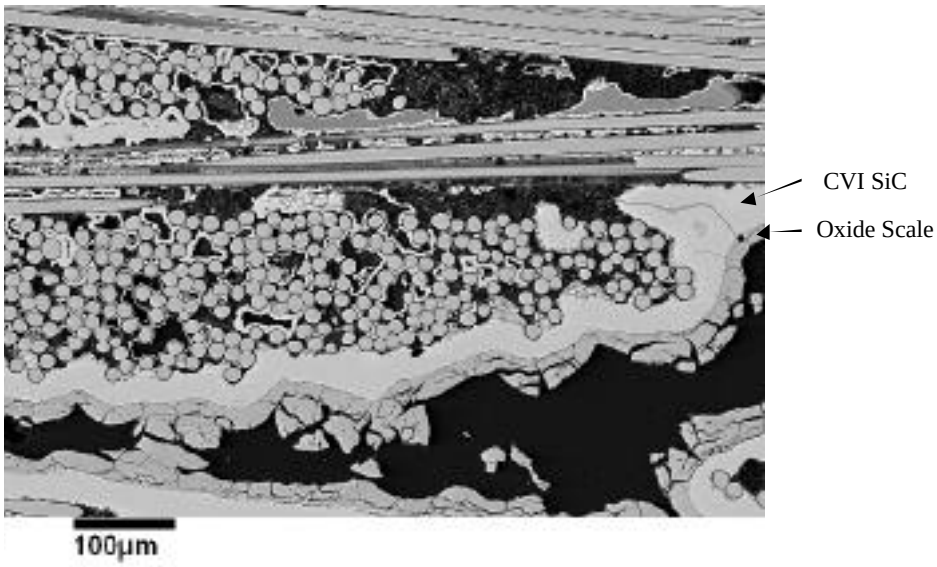

Figure 12 Cross-section of inner liner showing oxide scale on the internal SiC surfaces.

Conclusions

The exposure of SiC based ceramics in the HPTTF led to rapid oxidation. The silica scales were extensively damaged as reflected by the presence of cracks and pores. In terms of the porosity, the extent of this damage increased as the scale grew. In the case of the combustion environment, the high gas velocities lead to the volatilization of the silica scale.

For the case of the HPTTF tests, volatility effects could be neglected. The rate of oxidation was much higher than that predicted by extrapolating the data generated in Figure 1. This difference could in part be attributed to the ineffectiveness of the damaged silica scale as a diffusion barrier. Much better agreement was obtained by increasing the extrapolated value of the parabolic rate constant by a factor of 10.

The application of the paralinear oxidation model to experimental combustor liner results provided a good estimate of the SiC recession rate. However, the predicted value of the steady-state silica scale thickness, which depends upon the rate constants for both parabolic oxidation and linear volatilization, was significantly lower than the experimental value. Once again better agreement was obtained by increasing parabolic rate constant by a factor of 10. These results suggest that the silica scale volatility is fairly well described by Eq 3 while the oxidation data (Figure 1) tend to underestimate the parabolic rate constant when extrapolated to higher pressures.

Acknowledgements

This research was sponsored by the U. S. Department of Energy's Office of Industrial Technologies for the Advanced Turbine Systems Program, under contract DE-AC05-96OR22464 with Lockheed Martin Energy Research Corporation.

References

[1] Anson, D., Ramesh, K. S., and DeCorso, M., "Application of Ceramics To Industrial Gas Turbines"; Volume 1 Technology Background; Volume 2 Economics, Market

Analysis, and R&D Plan DOE/CE/40878-1&2; Battelle Columbus March 1991.

[2] Helms, H. E., Johnson, R. A., and Groseclose, L. E., "AGT 100-Advanced Gas Turbine Technology Development Project," pp. 137-55 in Proceedings of the Twenty-Third Automotive Technology Development Contractors' Coordination Meeting P-165, Society of Automotive Engineers,Warrendale, PA, March 1986.

[3] van Roode, M., "Ceramic Retrofit Program," pp. 77-93 in Proceedings of the Joint Contractors Meeting: FE/EE Advanced Turbine Systems Conference FE Fuel Cells and Coal-Fired Heat Engines Conference, DOE/METC-93/6132, August 1993.

[4] Carruthers, D. and Lindberg, L., "Critical Issues for Ceramics for Gas Turbines," pp 1258-1272 in Third International Symposium on Ceramic Components and Materials for Engines, edited by V. J. Tennery, American Ceramic Society, Westerville, Ohio, 1988.

[5] Haley, P. J., Holtman, R. L., Groseclose, L. E., Hilpisch, S. J., and Bell III, A. H., "Advanced Turbine Technology Applications Project [ATTAP)", pp 19-29 in Proceedings of the Twenty-Ninth Automotive Technology Development Contractors' Coordination Meeting, Society of Automotive Engineers, Warrendale, Penn., June 1992.

[6] Opila, E. J. and Hann, Jr., R. E., "Paralinear Oxidation of SiC in Water Vapor, " *Journal American Ceramic Society*, Vol. 80, No. 1, pp. 197-205, (1997).

[7] Opila, E. J., "Variation of the Oxidation Rate of Silicon Carbide with Vapor Pressure," *Journal American Ceramic Society*, Vol. 82, No. 3, pp. 625-36, (1999).

[8] Smialek, J. L., Robinson, R. C., Opila, E. J., Fox, D. S., and Jacobson, N., "SiC and Si_3N_4 Recession due to SiO_2 Scale Volatility Under Combustor Conditions, " *Advanced Composite Materials*, Vol. 8, No. 1, pp. 33-45, (1999).

[9] Keiser, J. R., Howell, M., and Pint, B. A., "Long-Term Corrosion of Ceramics in High Temperature Steam Environments," unpublished data, Oak Ridge National Laboratory, June 1998.

[10] More, K. L., Tortorelli, P. F., Ferber, M. K., Walker, L. R., Keiser, J. R., Brentnall, W. D., Miriyala, N., and Price, J. R., "Exposure of Ceramics and Ceramic Matrix Composites in Simulated and Actual Combustor Environments," to be presented at ASME TURBO EXPO '99, June 7-10, 1999, Indianapolis, Indiana.

[11] Luthra, K. L. "Some New Perspectives on Oxidation of Silicon Nitride and Silicon Nitride," *Journal American Ceramic Society*, Vol. 74, No. 5, pp. 1095-1103, (1991).